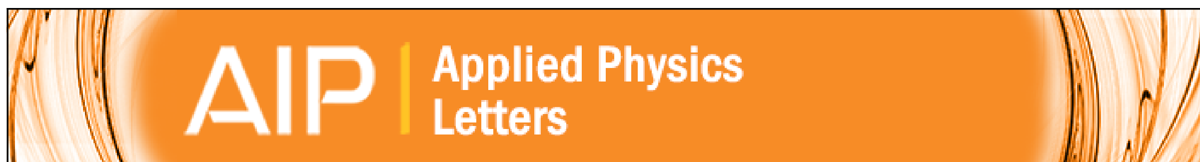

Flexoelectricity in barium strontium titanate thin film

Seol Ryung Kwon, Wenbin Huang, Longlong Shu, Fuh-Gwo Yuan, Jon-Paul Maria, and Xiaoning Jiang

Citation: Applied Physics Letters **105**, 142904 (2014); doi: 10.1063/1.4898139
View online: http://dx.doi.org/10.1063/1.4898139
View Table of Contents: http://scitation.aip.org/content/aip/journal/apl/105/14?ver=pdfcov
Published by the AIP Publishing

Articles you may be interested in

Effects of poling, and implications for metastable phase behavior in barium strontium titanate thin film capacitors
Appl. Phys. Lett. **85**, 5010 (2004); 10.1063/1.1827934

High tunability barium strontium titanate thin films for rf circuit applications
Appl. Phys. Lett. **85**, 4451 (2004); 10.1063/1.1818724

Ferroelectric properties of an epitaxial lead zirconate titanate thin film deposited by a hydrothermal method below the Curie temperature
Appl. Phys. Lett. **84**, 5094 (2004); 10.1063/1.1762973

Improvement in electrical characteristics of graded manganese doped barium strontium titanate thin films
Appl. Phys. Lett. **82**, 1911 (2003); 10.1063/1.1560861

Dielectric anomaly in strontium bismuth tantalate thin films
Appl. Phys. Lett. **73**, 1649 (1998); 10.1063/1.122234

AIP Chaos
CALL FOR APPLICANTS
Seeking new Editor-in-Chief

This article is copyrighted as indicated in the article. Reuse of AIP content is subject to the terms at: http://scitation.aip.org/termsconditions. Downloaded to IP: 152.14.118.175 On: Mon, 13 Oct 2014 14:27:02

Flexoelectricity in barium strontium titanate thin film

Seol Ryung Kwon,[1] Wenbin Huang,[1] Longlong Shu,[1,2] Fuh-Gwo Yuan,[1] Jon-Paul Maria,[3] and Xiaoning Jiang[1,a)]
[1]*Department of Mechanical and Aerospace Engineering, North Carolina State University, Raleigh, North Carolina 27695, USA*
[2]*Electronic Materials Research Laboratory, International Center for Dielectric Research, Xi'an Jiao Tong University, Xi'an, Shaanxi 710049, China*
[3]*Department of Material Science and Engineering, North Carolina State University, Raleigh, North Carolina 27695, USA*

(Received 15 August 2014; accepted 3 October 2014; published online 10 October 2014)

Flexoelectricity, the linear coupling between the strain gradient and the induced electric polarization, has been intensively studied as an alternative to piezoelectricity. Especially, it is of interest to develop flexoelectric devices on micro/nano scales due to the inherent scaling effect of flexoelectric effect. $Ba_{0.7}Sr_{0.3}TiO_3$ thin film with a thickness of 130 nm was fabricated on a silicon wafer using a RF magnetron sputtering process. The flexoelectric coefficients of the prepared thin films were determined experimentally. It was revealed that the thin films possessed a transverse flexoelectric coefficient of 24.5 μC/m at Curie temperature (~28 °C) and 17.44 μC/m at 41 °C. The measured flexoelectric coefficients are comparable to that of bulk BST ceramics, which are reported to be 10–100 μC/m. This result suggests that the flexoelectric thin film structures can be effectively used for micro/nano-sensing devices. © *2014 AIP Publishing LLC*.
[http://dx.doi.org/10.1063/1.4898139]

Direct flexoelectricity, referred to the generation of electric polarization response induced by a mechanical strain, is usually described as

$$P_l = \mu_{ijkl} \frac{\partial \varepsilon_{ij}}{\partial x_k}, \qquad (1)$$

where P_l is the component of flexoelectric polarization, μ_{ijkl} is the flexoelectric coefficients, a fourth rank tensor, ε_{ij} is the mechanical strain tensor, and x_k is the direction of the gradient in ε_{ij}. For a cubic crystal, μ_{ijkl} has three non-zero independent components μ_{1111}, μ_{1122}, and μ_{1212} or in matrix notation μ_{11}, μ_{12}, and μ_{44}.

The flexoelectricity in solid crystalline materials was first proposed approximately 50 years ago.[1] Later, it was demonstrated to be of great potential as an alternative of piezoelectricity. In crystallography, flexoelectricity is exhibited in all dielectric solids while piezoelectricity can only be found in non-centrosymmetric crystal systems (20 out of 32 point groups).[2–4] This feature widely broads the selection of materials for electromechanical sensing with preferable properties. On the other hand, the mechanism of the flexoelectricity results in the absence of poling process before using the flexoelectric material. Typically, the piezoelectric materials always age rapidly in the first few hours after removal of the poling field.[5,6] Unlike piezoelectric materials, the flexoelectric materials do not exhibit de-poling or poling related aging problems.[7] Intriguingly, it is also expected that flexoelectric materials can function at a broader range of temperatures over their piezoelectric counterparts, whose operating temperature is usually constrained within a small range near the Curie temperature. Moreover, the flexoelectric structures are also expected to exhibit high sensitivity when the structures are scaled down to micro/nano domains due to the scaling effect.[2,7–9]

A variety of dielectric materials have been studied for their flexoelectricity. Among all of the reported materials,[10–15] BST has garnered the most attention due to its largest flexoelectric properties at its Curie temperature of 21 °C. However, even when materials with high flexoelectric coefficients were utilized, sensors based on flexoelectricity in macro scale still exhibited lower sensitivities compared to piezoelectric counterparts.[16] To overcome the low sensitivities of flexoelectric sensors, a multilayered sensing structure[17] was developed by stacking up flexoelectric layers. However, fabricating these thin structures with electrodes connected in parallel is difficult.[17] Therefore, scaling down flexoelectric sensing structures seems to be necessary to enhance the performance of flexoelectric sensors.

In order to obtain flexoelectric BST micro/nano-sensors, top-down or bottom-up micro/nanofabrications can be adopted. However, it is challenge to utilize the BST bulk materials in the top-down process due to its fragility and low etching rate.[18] On the other hand, the bottom-up fabrication technique is preferred to the top-down technique because that deposition of thin film dielectric materials has been reported with successes. Among various thin film fabrication methods,[19–22] RF magnetron sputtering is favorable due to its ease of implementation, superior compositional reproducibility, controllability, good crystallinity, and desirable dielectric properties.

In this letter, a flexoelectric thin film structure was designed and fabricated using the RF magnetron sputtering process. The dielectric, piezoelectric, and flexoelectric properties of the fabricated BST thin film were characterized to determine the flexoelectric transverse coefficient of BST thin films using a bending method.

[a)]Electronic mail: xjiang5@ncsu.edu

 © 2014 AIP Publishing LLC

This article is copyrighted as indicated in the article. Reuse of AIP content is subject to the terms at: http://scitation.aip.org/termsconditions. Downloaded to IP: 152.14.118.175 On: Mon, 13 Oct 2014 14:27:02

A beam bending method was developed to characterize the flexoelectric properties of BST thin films as shown in Fig. 1(a). For pure bending of a beam with $L \gg b \gg t$, the flexoelectric polarization, in response to the gradient of axial normal strain ε_{11} in the thickness direction, can be simplified and written as Eq. (2).[23] Here, μ_{12}^{eff}, ν, z, and ε denote the effective transverse flexoelectric coefficient, the Poisson ratio of BST thin film, position coordinate in Z direction, and elastic strain, respectively

$$P_3 = \mu_{11}\frac{\partial \varepsilon_{33}}{\partial z} + \mu_{12}\left(\frac{\partial \varepsilon_{11}}{\partial z} + \frac{\partial \varepsilon_{22}}{\partial z}\right) = \left[\nu\mu_{11} + (1+\nu)\mu_{12}\right]\frac{\partial \varepsilon_{11}}{\partial z} = \mu_{12}^{eff}\frac{\partial \varepsilon_{11}}{\partial z}. \quad (2)$$

From the Euler-Bernoulli beam theory, the strain gradient can be calculated as[24]

$$\frac{\partial \varepsilon_{11}}{\partial z} = \frac{\partial^2 w(x)}{\partial x^2} = \frac{F(L-x)}{EI}, \quad (3)$$

where E and I are the Young's modulus and the moment of inertia of the substrate, respectively. Then, the polarization P_3 can be obtained by substituting Eq. (3) into (2) and the total induced charge Q can be calculated by integrating the polarization along the beam length direction.

$$Q = \int P_3 dA = \mu_{12}^{eff}\frac{\pi r^2 F(L-l)}{EI} = \mu_{12}^{eff}\frac{3\pi r^2 \delta(L-l)}{L^3}. \quad (4)$$

Finally, the transverse flexoelectric coefficient μ_{12}^{eff} can be calculated from the output charge and the displacement at the tip. The dimensions and material properties of the structure are shown in Table I.

$$\mu_{12}^{eff} = \frac{QL^3}{3\pi r^2 \delta(L-l)}. \quad (5)$$

The BST thin film was prepared by RF magnetron sputtering using a $Ba_{0.7}Sr_{0.3}TiO_3$ target. 22.5 nm of SiO_2 layer

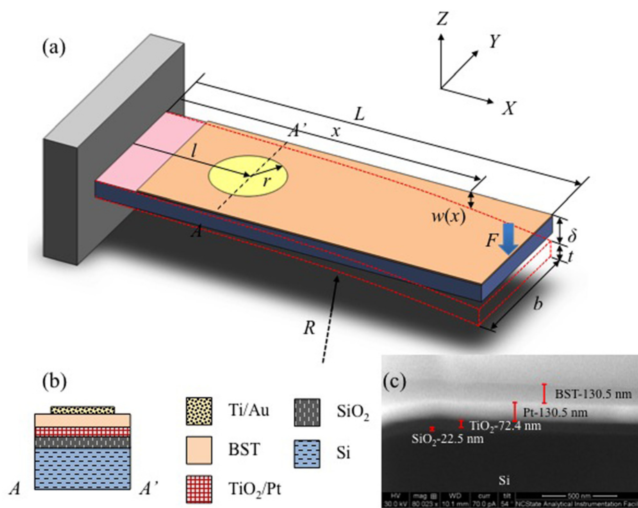

FIG. 1. (a) The configuration of a BST thin film cantilever. (b) Cross-section view across A and A', (c) Cross-section SEM picture of the BST thin film (x: axial distance from the clamped end, $w(x)$: deflection at x, F: applied force at the tip, L: beam length, δ: tip deflection, r: radius of top electrode and l: distance from the base of cantilever to the center of the top electrode).

TABLE I. The dimensions and material properties of the BST thin film cantilever.

L (mm)	l (mm)	r (μm)	t_{Si} (μm)	t_{BST} (nm)	E_{Si} (GPa)	E_{BST} (GPa)
7.43	4.45	320	525	130.5	125.5	185.0

and bottom electrode of TiO_2/Pt (72.4 nm/130 nm) were deposited on a silicon wafer sequentially. The film was deposited with rate of 0.0181 Å/s at 300 °C with a shadow mask to expose some area of the bottom electrode for electrical connection. Later, it was post annealed in air at 700 °C for 20 h. Finally, a top electrode of Ti/Au (10 nm/100 nm) was deposited in a circular shape using a shadow mask. The structure of thin film is schematically shown in Fig. 1(b). The microstructure and crystallization of the BST thin film were examined by a scanning electron microscopy (JEOL, JSM-6400F) and an X-ray diffractometer (Rigaku, SmartLab) with Cu Kα radiation ($\lambda = 0.15406$ nm) operating at 40 kV and 100 mA, respectively. The SEM picture of the cross section is illustrated in Fig. 1(c). The thickness of the BST thin film was measured to be 130.5 nm. The XRD pattern of the BST thin film deposited on Pt(111)/TiO_2/SiO_2/Si(100) is shown in Fig. 2. The pattern matches very well with previously reported works.[25,26]

The capacitance of the BST thin film was measured at 1 kHz by an impedance analyzer (Agilent, 4294 A). Fig. 3 shows the temperature dependence of the dielectric constant and the dielectric loss tangent. It was observed that the dielectric constant of the BST thin film (327) is much lower than bulk BST (e.g., 8000 at room temperature). In principle, thicker film has a larger dielectric constant due to larger size of grains. Similarly, small grain size increases grain boundaries, resulting in higher leakage current and lower dielectric constant.[20] Around 28 °C (Curie temperature), a transition from the ferroelectric phase to the paraelectric phase is noted. The broad peak in the response of ferroelectric films can be attributed to the mechanical and electrical strains in the films. These strains cause different grains to have different transition temperatures and a non-ferroelectric surface

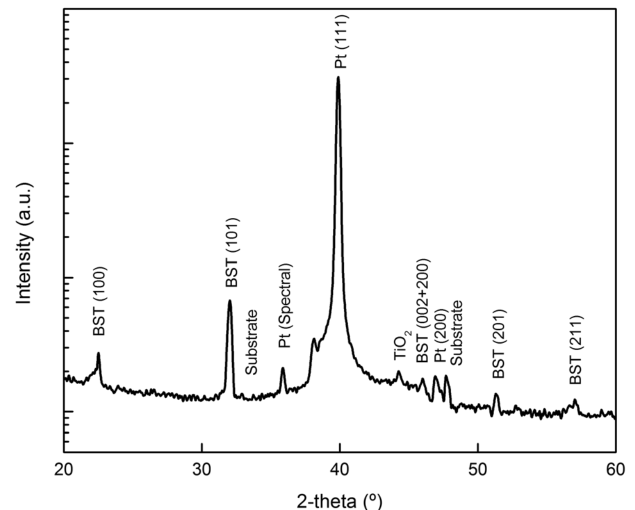

FIG. 2. XRD pattern of RF sputtered $Ba_{0.7}Sr_{0.3}TiO_3$ thin film deposited on Pt.

This article is copyrighted as indicated in the article. Reuse of AIP content is subject to the terms at: http://scitation.aip.org/termsconditions. Downloaded to IP: 152.14.118.175 On: Mon, 13 Oct 2014 14:27:02

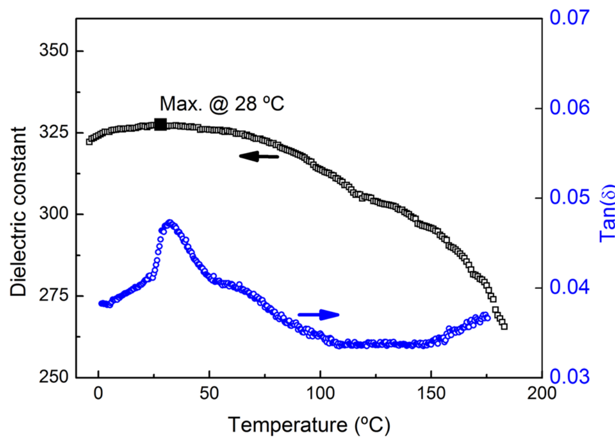

FIG. 3. Dielectric constant and dielectric loss of BST thin film at different temperatures.

layer at the grain boundaries and on the surface of the film.[27] The dielectric loss is less than 5% throughout the entire measurement temperature range.

The topography and surface piezoelectric response of the BST thin film was measured by a piezoresponse force microscopy (PFM) (Asylum, MFP-3D) at room temperature as shown in Fig. 4. It is noticed that the BST thin film is in its ferroelectric state at room temperature so that the piezoelectricity might be present in this state even though the film had not been poled. The effective piezoelectric coefficient d_{33} of the BST thin film was measured using a Pt-coated PFM tip under a 4 V AC excitation. As shown in Fig. 4(a), the PFM amplitude results indicate that the fabricated BST thin film exhibits a small localized piezoelectricity with a maximum piezoelectric constant of about 3 pm/V. At the same time, no 180° phase contrast was found in the PFM phase as shown in Fig. 4(b). With the help of PFM, it is reasonable to evaluate the global piezoelectric coefficient of the thin film by averaging the measured responses over the whole area, which should be even smaller than the maximum measured value ($d_{33} \sim 3$ pm/V).[28]

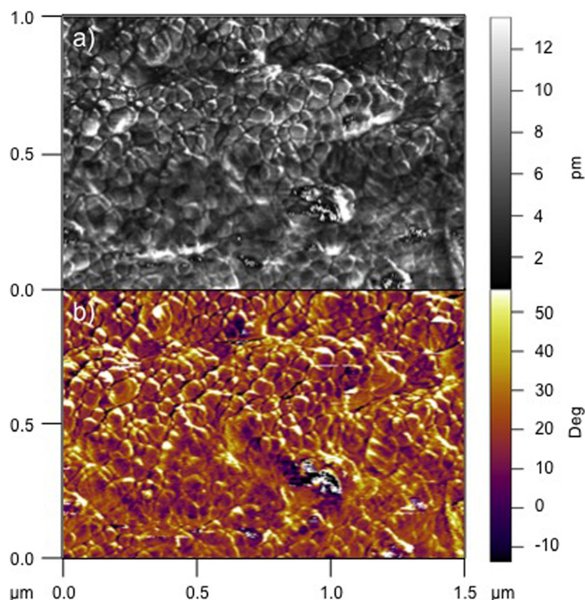

FIG. 4. The topography and piezoelectricity of BST thin film measured under room temperature. (a) Magnitude. (b) Phase.

Furthermore, the contribution of piezoelectricity in d_{31} mode was also measured. For this test, a 10 V AC excitation was applied across the top and bottom electrodes at room temperature. The generated displacement at the tip of the cantilever was undetectable by a laser vibrometer (Polytec, OFV-5000) with resolution of 10 pm. A calculation for corresponding d_{31} for this case was performed, and it indicated a maximum d_{31} value of 17.8 fm/V. The piezoelectric proportion in the total charge output under bending test was calculated to be 0.01%, suggesting the electric output of the bending test is dominantly attributed to the flexoelectricity of the BST thin film.

The measurement of the effective μ_{12} coefficient was measured by bending the substrate described by Huang *et al.*[2] It was carried out in a thermal chamber. The flexoelectric beam structure was clamped rigidly at one end and deflected by a piezoelectric actuator at the tip. The actuator was driven by a power amplifier (Brüel & Kjær, type 2706) under a 2 Hz-excitation from a function generator (Tectronix, Model AFG3101). It is worth mentioning that the selection of the frequency is much lower than the resonance frequency of the cantilever beam and therefore the displacement does not significantly differ from the static case for beam deflection model derivation. The deflection of the cantilever was measured by a laser vibrometer (Polytec, OFV-5000). The generated charge signal was measured by the combination of a charge amplifier (Brüel & Kjær, type 2635) and a lock-in amplifier (Stanford Research system, Model SR830). The transverse flexoelectric coefficient μ_{12}^{eff} was calculated from the charge output and tip deflection using Eq. (5).

In order to ensure all the output signals being derived from the materials rather than the system noise, a contrast test with a silicon cantilever without BST thin film was performed. It was fabricated into the identical size to verify if the measured charge output was noise current or purely came from flexoelectricity. Under 1 μm tip excitation of 2 Hz, the measured charge output was almost 0 C and the phase of the charge output was unlocked to the input frequency of the tip excitation. This means the charge output from the cantilever was not coupled from piezoelectricity. Thus, the measured charge output from the silicon cantilever was a noise current, and it was not significant when μ_{12} of BST thin film is measured.

As seen in Fig. 5, μ_{12} of BST thin film was measured at different temperature from 24 to 41 °C. The temperature was converted to dielectric constant in the insect of Fig. 5. At all measured temperatures, the strain gradient and electric polarization have linear relationship. Fig. 6 shows the measurement points of three trials and average μ_{12} (slope). At paraelectric phase (41 °C), which is above the Curie temperature (28 °C), the BST thin film still possess high μ_{12} of 17.44 μC/m.

Although the dielectric constant of BST thin film was much smaller than that of BST ceramics, the magnitude of the flexoelectric constant of the BST thin film is comparable to that of BST bulk material. We suggest several reasons for this phenomenon. One reason might be that the low

This article is copyrighted as indicated in the article. Reuse of AIP content is subject to the terms at: http://scitation.aip.org/termsconditions. Downloaded to IP: 152.14.118.175 On: Mon, 13 Oct 2014 14:27:02

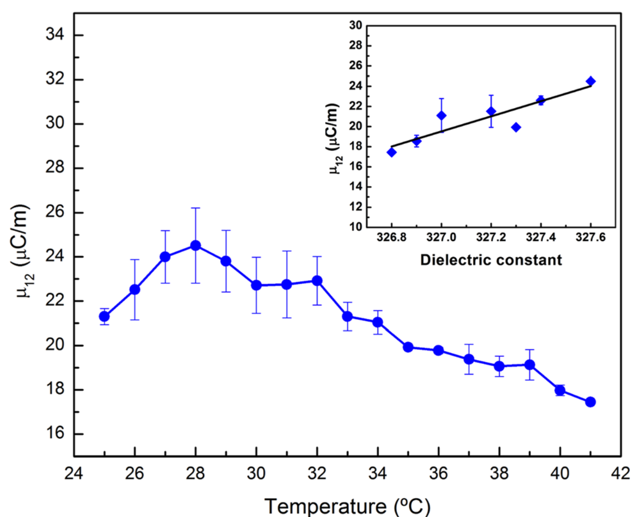

FIG. 5. Temperature dependence of the transverse flexoelectric coefficient of BST. Inset: the transverse flexoelectric coefficients as a function of dielectric constant.

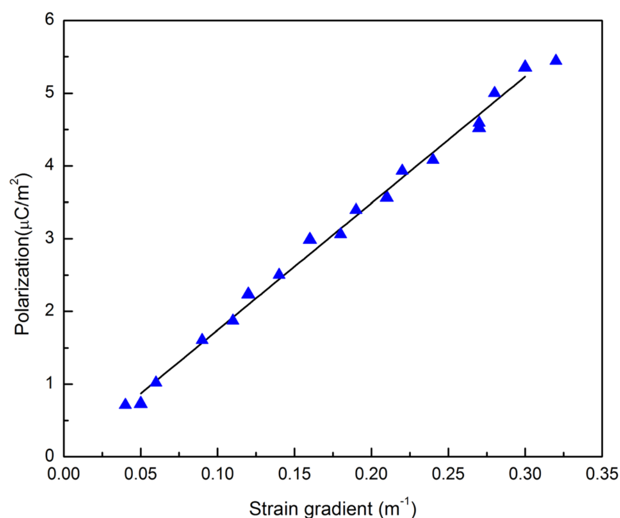

FIG. 6. Flexoelectric polarization as a function of applied strain gradient measured at 41 °C and flexure frequency of 2 Hz.

dielectric constant of the BST thin film is largely attributed to its small grain size configuration, which generates vast numbers of grain boundaries and incurs a tremendous external pinning effect. However, the inner atomic structure was not affected by the small grain size. This suggests that the strain gradient induced mismatch of positive and negative charge centroids remained the same, thus producing the same level of flexoelectric polarization as bulk materials. Another possibility lies in the lattice mismatch and annealing,[29] which can results in residual stress in thin films. In the presence of residual stress, the relaxation along the thickness direction would cause an extremely high strain gradient compared with the bulk mechanical test.[30] The mechanism of how it affects on flexoelectricity has not been clearly explained yet. However, the high intrinsic strain gradient in the BST thin film may cause the flexoelectricity more sensitive to the external strain gradient.

In summary, enhanced flexoelectric effect was observed in $Ba_{0.7}Sr_{0.3}TiO_3$ thin film. The measured effective transverse flexoelectric coefficient μ_{12}^{eff} was found to be 24.5 μC/m at Curie temperature (28 °C) and 17.44 μC/m at 41 °C, which is comparable to that of bulk BST ceramics. This result ensures the feasibility of enhanced flexoelectricity in micro/nano domains without sacrificing large flexoelectric coefficients. With proper design, the BST thin film is possible to be used in flexoelectric micro/nano scale sensing devices, which are preferable to macroscale devices due to the flexoelectric scaling effect.

This work was supported by, or in part by, the U.S. Army Research Laboratory and the U.S. Army Research Office under Contract/Grant No. W911NF-11-1-0516; and in part by National Science Foundation under Grant No. CMMI-1068345.

[1]S. M. Kogan, Sov. Phys. Solid State **5**, 2069 (1964).
[2]W. Huang, K. Kim, S. Zhang, F.-G. Yuan, and X. Jiang, Phys. Status Solidi RRL **5**, 350 (2011).
[3]X. Jiang, W. Huang, and S. Zhang, Nano Energy **2**, 1079 (2013).
[4]L. Shu, W. Huang, S. R. Kwon, Z. Wang, F. Li, X. Wei, S. Zhang, M. Lanagan, X. Yao, and X. Jiang, Appl. Phys. Lett. **104**, 232902 (2014).
[5]P. Glynne-Jones, S. Beeby, and N. White, Meas. Sci. Technol. **12**, 663 (2001).
[6]J. F. Shepard, F. Chu, I. Kanno, and S. Trolier-McKinstry, J. Appl. Phys. **85**, 6711 (1999).
[7]W. Huang, S.-R. Kwon, S. Zhang, F.-G. Yuan, and X. Jiang, J. Intell. Mater. Syst. Struct. **25**, 271 (2014).
[8]M. Majdoub, P. Sharma, and T. Cagin, Phys. Rev. B: Condens. Matter **77**, 125424 (2008).
[9]T. D. Nguyen, S. Mao, Y. W. Yeh, P. K. Purohit, and M. C. McAlpine, Adv. Mater. **25**, 946 (2013).
[10]L. Shu, X. Wei, L. Jin, Y. Li, H. Wang, and X. Yao, Appl. Phys. Lett. **102**, 152904 (2013).
[11]W. Ma and L. E. Cross, Appl. Phys. Lett. **86**, 072905 (2005).
[12]W. Ma and L. E. Cross, Appl. Phys. Lett. **88**, 232902 (2006).
[13]W. Ma and L. E. Cross, Appl. Phys. Lett. **78**, 2920 (2001).
[14]P. Zubko, G. Catalan, A. Buckley, P. Welche, and J. Scott, Phys. Rev. Lett. **99**, 167601 (2007).
[15]B. Chu and D. R. Salem, Appl. Phys. Lett. **101**, 103905 (2012).
[16]W. Huang, X. Yan, S. R. Kwon, S. Zhang, F.-G. Yuan, and X. Jiang, Appl. Phys. Lett. **101**, 252903 (2012).
[17]S. Kwon, W. Huang, S. Zhang, F. Yuan, and X. Jiang, Smart Mater. Struct. **22**, 115017 (2013).
[18]R. Zhang, C. Yang, A. Yu, B. Wang, H. Tang, H. Chen, and J. Zhang, Appl. Surf. Sci. **254**, 6697 (2008).
[19]D. Ghosh, B. Laughlin, J. Nath, A. Kingon, M. Steer, and J. P. Maria, Thin Solid Films **496**, 669 (2006).
[20]S. M. Aygun, J. F. Ihlefeld, W. J. Borland, and J. P. Maria, J. Appl. Phys. **109**, 034108 (2011).
[21]J. G. Cheng, X. J. Meng, B. Li, J. Tang, S. L. Guo, J. H. Chu, M. Wang, H. Wang, and Z. Wang, Appl. Phys. Lett. **75**, 2132 (1999).
[22]S. I. Jang and H. M. Jang, Thin Solid Films **330**, 89 (1998).
[23]W. Ma, Phys. Status Solidi B **245**, 761 (2008).
[24]A. C. Ugural and S. K. Fenster, *Advanced Mechanics of Materials and Applied Elasticity* (Pearson Education, 2011).
[25]T. Zhang and H. Ni, Sens. Actuators, A **100**, 252 (2002).
[26]D. Wang, Y. Wang, X. Zhou, H. Chan, and C. Choy, Appl. Phys. Lett. **86**, 212904 (2005).
[27]S. Lahiry and A. Mansingh, Thin Solid Films **516**, 1656 (2008).
[28]E. Soergel, J. Phys. D: Appl. Phys. **44**, 464003 (2011).
[29]G. Catalan, A. Lubk, A. Vlooswijk, E. Snoeck, C. Magen, A. Janssens, G. Rispens, G. Rijnders, D. Blank, and B. Noheda, Nat. Mater. **10**, 963 (2011).
[30]G. Catalan, L. Sinnamon, and J. Gregg, J. Phys. Condens. Matter **16**, 2253 (2004).

This article is copyrighted as indicated in the article. Reuse of AIP content is subject to the terms at: http://scitation.aip.org/termsconditions. Downloaded to IP: 152.14.118.175 On: Mon, 13 Oct 2014 14:27:02